DEAD FUEL MOISTURE CONTENT ESTIMATION USING REMOTE SENSING

Konstantinos ZORMPAS
University of the Aegean, Department of Geography, Mytilene, Greece
geo12045@geo.aegean.gr

Christos VASILAKOS
University of the Aegean, Department of Geography, Mytilene, Greece
http://vasilakos.aegean.gr/
chvas@aegean.gr

Nikos ATHANASIS
University of the Aegean, Department of Geography, Mytilene, Greece
athanasis@geo.aegean.gr

Nikos SOULAKELLIS
University of the Aegean, Department of Geography, Mytilene, Greece
http://cartogi-lab.aegean.gr/index.php/GR/
nsoul@aegean.gr

Kostas KALABOKIDIS
University of the Aegean, Department of Geography, Mytilene, Greece
http://catastrophes.geo.aegean.gr/
kalabokidis@aegean.gr

Abstract

One of the critical parameters in wildfire behavior is the dead fuel moisture content (DFMC). DFMC is affected from environmental factors and the vegetation characteristics, thus it varies across the landscape. Previous research showed that remote sensing reflectance data can assist the spatial estimation of DFMC. The aim of this paper is to evaluate the Landsat 8 in retrieving the DFMC in a complex Mediterranean ecosystem. The Normalized Difference Vegetation Index (NDVI) and the top of atmosphere brightness temperature are correlated with the 10-h fuel moisture content and the surface temperature recorded from Remote Automatic Weather Stations (RAWS). Training data are collected from the year 2015 and the validation is applied to year 2016. According to the literature, the DFMC was correlated with the ratio of NDVI/LST, however, our results were not satisfactory producing low r^2 coefficients. New models were developed based on the DFMC and the brightness temperature (BT) which resulted to r^2 values up to 0.733. The validation with new data confirmed that the top of atmosphere brightness temperature retrieved from Landsat 8, can be used as an input to estimate the spatial distribution of DFMC. The process was fully automated, i.e. from data ordering to map preparation, and is ready to continually provide the wildfire managers and firefighting personnel confronting wildfires with the DFMC maps.

Keywords*: 10-hour dead fuel moisture content, forest fires, remote sensing, brightness temperature (BT), Landsat*

1. INTRODUCTION

The significant influence of the fuel moisture content (FMC) in wildfires, has been recognized by wildfire managers and scientists (Pollet and Brown, 2007). Fire behavior has great sensitivity to water content which is a key parameter in risk assessment (Vejmelka et al., 2016). Since forest fires affect a large variety of vegetation and ecosystems, scientists began to develop various fire danger rating models and the FMC is one of the parameters that is taken into consideration. Various physical and environmental factors influence moisture content and many authors managed to identify the major conditions that influence the water content (Dimitrakopoulos and Papaioannou, 2001; Verbesselt et al., 2006; Danson and Bowyer, 2004; Chuvieco et al., 2002; Aguado et al., 2007). Dimitrakopoulos and Papaioannou (2001) stated that water content is related in inversion to the probability of inflammation, because part of the heat required to begin a fire is used from the evaporation process. Additionally, slow fire spread appears on vegetation with high moisture content since the source of the flames is reduced when there are wet materials (Aguado et al., 2007) and because part of the heat released by the fire front is used to absorb water from fuels nearby (Chuvieco et al., 2002).

There are many methods for estimating FMC (Pinto et al., 2014). However, the most common technique comes from the equation (1) which describes the ratio of weight of the water in the sample or material to the dry weight of the sample (Countryman and Dean, 1979):

$$FMC = \left(\frac{W_w - W_d}{W_d}\right) \times 100 \qquad (1)$$

where, W_w is fresh weight and W_d is the dry weight but generally it is expressed as the percentage of leaf dry weight (Chuvieco et al., 2004a; Danson and Bowyer, 2004). The above equation requires field samples and their weight is determined in the laboratory. In wildfire behavior, it is critical to know both the live and dead fuel moisture content (DFMC) (Danson and Bowyer, 2004). The DFMC can be found in branches that are categorized according to their size, in leaves and pine needles lying on the ground and in any dead vegetation. At each interval (1, 10, 100, 1000 hrs) fuel loses 63% moisture of the difference between the initial moisture content and the equilibrium moisture content (Pollet and Brown, 2007). Other estimation methods of DFMC are by using meteorological indices (Aguado et al., 2007), and the inversion of the radiative transfer equation (Riaño et al., 2005). Although field sampling and measurements are expensive and consume time, they are accurate at local level (Chuvieco et al., 2004a; Sow et al., 2013). Additionally, retrieving the spatial distribution based on these point measurements is not feasible (Yebra et al., 2013). Remote Automatic Weather Stations (RAWS) are used for retrieving 10-h fuel moisture by pine dowel that emulates the moisture content of similarly sized twigs on the forest floor. Unlike DFMC, the estimation of live fuel moisture content is more difficult (Viegas et al., 2001) although dead fuels are more dangerous because they are drier than live and respond faster on rapid changes of the atmosphere (Chuvieco et al., 2004b).

The drawbacks described previously, can be overcome by using satellite remotely sensed data (Chuvieco et al., 2004a). The increasing technology of observation instruments can provide significant estimations not only for moisture and fire monitoring but for other environmental conditions (Gerdzheva, 2014). By using satellites, researchers can estimate directly vegetation status, in which water stress, affects vegetation electromagnetic behavior, because images cover the whole area of interest (Prosper-Laget et al., 1995). Although remote sensing is considered an advantage on DFMC estimation, satellites on the other hand have their own characteristics. For example, as Verbesselt et al., (2006) stated, satellites like Landsat, with high spatial resolution, provide precise information of vegetation like fuel types but have low temporal resolution unlike satellites like NOAA-AVHRR or MODIS which revisit period is shorter than the one of Landsat. That means there could be a regular update of information about vegetation water stress, considering that water content temporal frequency can vary significantly (Sow et al., 2013). In general, remote sensing of vegetation monitoring can provide an alternative instant way for detecting water condition.

Most researchers are based on both the optical and thermal part of the electromagnetic spectrum, using the reflectance properties of vegetation. Sow et al. (2013) have shown that many authors use the combined information of different wavelengths. However, the most important element with plant reflectance is that remote sensing is able to discriminate the affection of water content from factors like other vegetation characteristics and soil below plants (Yebra et al., 2013). Many studies have shown that SWIR (short-wave infrared) is the most sensitive channel to water absorption (Chuvieco, 2009). However, for vegetation analysis the best approach is the usage of vegetation indices (Sow et al., 2013) and the most common of them is NDVI when analyzing it at multi-temporal series (Alonso et al., 1996). NDVI was proposed for the first time from Rouse et al. (1973) and is described by the following equation:

$$NDVI = \frac{NIR - RED}{NIR + RED} \qquad (2)$$

where NIR and RED are the reflectances of near infrared and visible red, respectively. It is assumed that NDVI is sensitive to water content changes, since it estimates chlorophyll activity and vegetation vigor (Chuvieco et al., 2004a). For example, Ceccato et al. (2001) assumed that NDVI and FMC may be related because of the strong correlation between leaf chlorophyll content and leaf moisture content (Pettorelli, 2013). However, many researchers disagree about the direct measurement of vegetation water content from NDVI. Although they use vegetation indices as a proxy for indirect water stress detection, the connection between FMC and chlorophyll is not direct since it depends on plant species and their phenological status, atmospheric pollution, nutrient deficiency, toxicity, plant disease and radiation stress (Ceccato et al., 2001; Dasgupta et al., 2005). Usually, this approach to retrieve FMC though NDVI, is done when estimating live FMC but when measuring DFMC through remote sensing it is difficult because dead fuels do not have variations in chlorophyll of leaves and weather affects water alternations (Verbesselt et al., 2006). On the other hand, plant drying causes a decrease in leaf area index (LAI) and chlorophyll content, so FMC could be indirectly measured as the result of the effects from this procedure. Conclusively, positive linear correlations reported using real FMC data and satellite derived NDVI (Jones and Reinke, 2009).

Similar approaches were made from Gao (1996), who used NIR and SWIR bands to propose NDWI (Normalized Difference Water Index). The basic concept about using NIR is that plants have high reflectance in this part of the spectrum (Jones and Reinke, 2009) and indices using NIR and SWIR estimate water content directly, since they comprehend wavelengths that are related more to water absorption channels. Several other studies (Alonso et al., 1996; Dasgupta et al., 2005; Hong and Lakshmi, 2007; Prosper-Laget et al., 1995; Sow et al., 2013) extended the use of different indices analyzing the combination of NDVI and LST making temperature measurements significant on vegetation water stress detection. As Sow et al. (2013) stated, "the primary basis for this relationship should be found in the unique spectral reflectance-emittance properties of plant leaves in the red and infrared wavelengths combined with the low thermal mass of plant leaves relative to soil". Also, soil moisture and thus NDVI reduction is due to the increase of evapotranspiration caused from temperature rise (Sun and Kafatos, 2007). In addition, there is a negative correlation between NDVI and LST. Water stress can rise rapidly the surface temperature (Wan et al., 2004). A connection between drying of plants and rise of the temperature has also been reported from measurements of the thermal spectrum, caused by evapotranspiration variations. LST is an important parameter in understanding the physics of the earth's surface process (Li et al., 2013) to model accurately the surface energy budget (Prata et al., 1995) and to understand the environmental phenomena such as forest fire danger and vegetation status (Hazaymeh et al., 2015).

Finally, a number of studies based on the relation between FMC real data and satellite indices have been proposed to estimate water content and showed good correlations, especially FMC with NDVI and LST. On the other hand, good results achieved from the combination of real FMC data and satellite derived indices may be plant species dependent (Chuvieco, 2009). For example, Chuvieco et al. (2004a), used a regression model combining FMC with NDVI and LST , to evaluate the connection between real ground FMC and satellite data at Canaberos Park in Spain. They found positive correlation and, as they stated, plant drying reduces chlorophyll activity.

The aim of this research is to examine the correlation between DFMC and the NDVI, the BT and the LST by using data retrieved from Landsat 8 and RAWS. DFMC and LST data are provided by RAWS of Lesvos Island while NDVI and BT are retrieved by the Landsat 8 image processing. General linear regression models were developed based on 2015 data and the model that provided the best statistics was validated with 2016 data producing a series of DFMC maps. The whole process was automated by developing a software that automatically downloads the satellite images from the USGS repository and creates the FMC maps in a transparent way to the end user.. FMC maps are available for browsing and downloading through an appropriate Web-GIS interface.

2. DATA AND METHODOLOGY

2.1 Study area

The island of Lesvos is located at the northeastern Aegean Sea of Greece and covers an area of 1636 km^2 with a variety of geological formations, climatic conditions and vegetation types (Figure 1). The terrain is rather hilly and rough, with its highest peak at 960 m. The soils of Lesvos are widely cultivated, mainly with rain-fed crops such as olive trees on the central, south and east parts of the island. These lands face frequent and low-intensity fire events due to their cultivation and land-cleaning practices. The vegetation of Lesvos Island, defined on the basis of the dominant species, includes phrygana or garrigue-type shrubs in grasslands; evergreen-sclerophylous or maquis-type shrubs; pine forests; deciduous oaks; olive tree groves; and other agricultural lands. The climate is typical Mediterranean, with warm and dry summers and mild and moderately rainy winters. The average annual air temperature is 18^0 C with high oscillations between maximum and minimum daily temperatures. Figure 2 shows the variation of the average monthly10-h Fuel Moisture Content during 2015. The vegetation water stress is high between April and September, while in July and August the 10-h fuel moisture is approximately 6%.

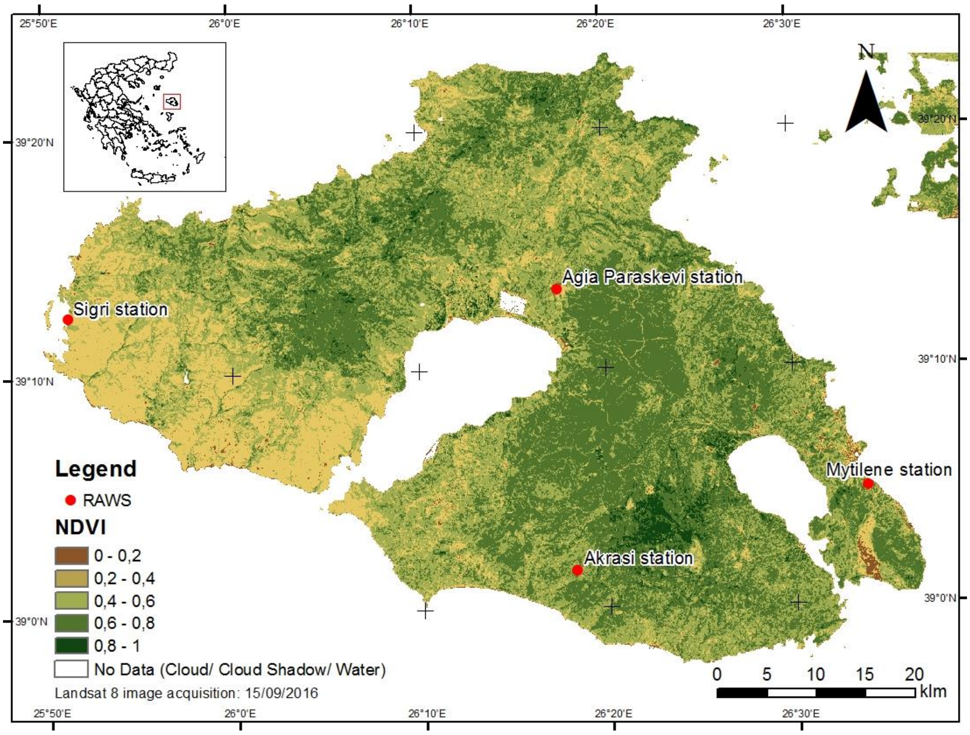

Figure 1: The study area of Lesvos Island, Greece.

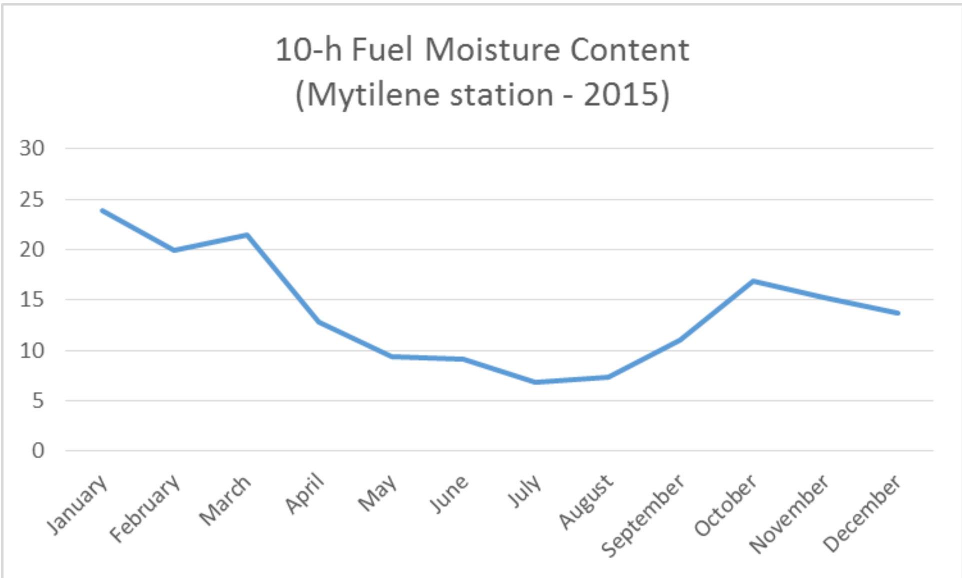

Figure 2: Annual variation of average monthly 10-h Fuel Moisture Content.

2.2 Data

Landsat 8 images (path:181, row:33) from the fire prevention periods of 2015 (1 May to 31 October 2015) and 2016 were used for this study. Landsat 8 is equipped with two sensors: OLI (Operational Land Imager) and TIRS (Thermal InfraRed Sensor). OLI collects data on nine multispectral bands (including the new Coastal/Aerosol and Cirrus) with a spatial resolution of 30 m. (with panchromatic band at 15 m) and TIRS with two thermal infrared bands. Landsat images were acquired from USGS as ready Landsat Surface Reflectance High Level Data Products i.e. the NDVI was based on the surface reflectance and the brightness temperature (at top of atmosphere) (Masek et al, 2006, Vermote et. al. 2016). Moreover, the cloud mask product was used for masking anything else but clear land. The data of the 2015 period was used for the training stage while the data of 2016 for the validation.

Meteorological data, used for this study, are provided by the Remote Automatic Weather Stations network installed and maintained by University of the Aegean, Greece (http://meteo.aegean.gr/). Out of the seven installed RAWS in Lesvos Island, only four of them provide 10-h FMC and three of them the land surface temperature (Figure 1). Therefore, from the satellite images the NDVI, BT1 (TIRS channel 1) and BT2 (TIRS channel 2) values were extracted from the 4 pixels of the RAWS, and for the same days and hour of image acquisitions the 10-h FMC and the LST values from the RAWS archive.

2.3 Methodology

To estimate the DFMC from the satellite images, simple linear regression models were developed based on previous research. The response variable was the DFMC and the explanatory variable were the NDVI, BT and LST. Based on the approach proposed by Chuvieco et al. (2004a), one of the correlations that were examined was the fuel moisture content with NDVI-LST. As mentioned before, NDVI and LST have greater influence on FMC when used together than separately usually by using their ratio (Eq. 3)

$$DFMC = a + b \times \frac{NDVI}{LST} \qquad (3)$$

However, instead of retrieving LST by the atmospheric correction of the Landsat thermal bands, the specific variable was replaced with the equation resulting from the correlation between LST and BT. Therefore, the equation 3 becomes:

$$DFMC = a + b \times \frac{NDVI}{c + d \times BT_x} \qquad (4)$$

Both of the thermal bands were tested in the correlation with the LST readings from RAWS. Except from the equation 4, more regression models were tested to correlate the DFMC with NDVI, LST and BT:

$$DFMC = a + b \times LST \qquad (5)$$
$$DFMC = a + b \times NDVI \qquad (6)$$
$$DFMC = a + b \times BT1 \qquad (7)$$
$$DFMC = a + b \times BT2 \qquad (8)$$

The purpose of the variable correlation is to find if the results of the regression are statistically significant. Equations 7 and 8 were tested only after the previous correlations did not resulted as expected and they were rejected. Before applying the regression between the variables, it was decided to check the data to find if there are deviations and outliers. In the graphs created for this purpose, it was found that July was the only month with deviation between the variables and was considered that it will not affect the correlations.

After the regression modelling, the most significant results were chosen and the final equation for the DFMC estimation was applied and validated. The aim was to validate the results with data that were not taken into consideration during the training phase and to produce the cartographic products that can be used by wildfire managers. For this reason 9 new Landsat 8 images were downloaded from May to October 2016. The DFMC values of the pixels corresponding to the RAWS locations were extracted. The estimated DFMC values and the actual 10-h Fuel Moisture Content readings were compared in order to compute the Root Mean Square error and to create a residual plot.

The DFMC maps are automatically generated in a transparent way to the end user by a software component based on the API of the ESPA Ordering System. The API provides the necessary functionality to programmatically determine available Landsat data distributed by the U.S. Geological Survey (USGS), place new orders and download the data when the order has been completed. The software component is running as a process that utilizes curl scripts triggered by a time scheduler at the time when new products from the USGS repository are available. When a new order has been placed, its status is continuously checked until the order completion.

Upon completion of the order, the order products are automatically downloaded and extracted. Then, a python script reads the mask file (cfmask.tiff) and the BT1 files from the downloaded order products and generates the DFMC geotiff files. Creation of DFMC maps includes: i) masking the water, cloud, cloud shadow and snow to NADATA, based on the CFMASK layer; ii) convert Kelvin to Celsius values; iii) calculation of DFMC; iv) project from WGS84 to GGRS87; and v) clip the study area. The DFMC maps are then automatically uploaded in the Web-GIS interface. The Web-GIS interface provides access to the available FMC files where end users can view or download. Figure 3 demonstrates the information flow for the creation of the FMC files.

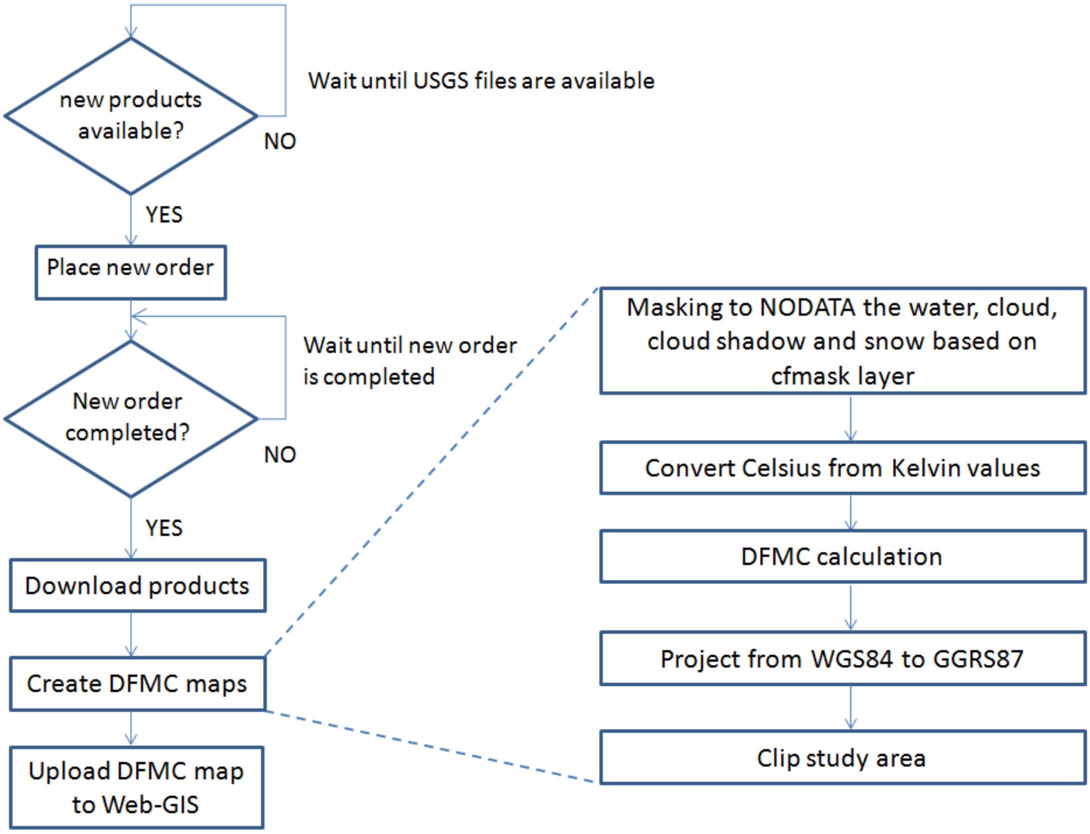

Figure 3: Process flow chart for the automatic DFMC preparation.

3. RESULTS AND DISCUSSION

3.1 Linear regression modelling

Two linear regression models were applied for the correlation between LST and BT1,BT2. The coefficient of determination r^2 was found sufficiently low, i.e. r^2 = 0.248 for BT1 and r^2 = 0.181 for BT2 (Figure 4a and 4b). This low estimation is due to the factors affecting brightness temperature that is different than actual surface temperature and is described below. The relationship between FMC and LST also resulted in a low value of r^2 = 0.3, although the linear relationship was negative confirming the hypothesis in the introduction (Figure 4c). The reason for this negative relationship is due to high temperatures that equal to increase of water loss (Chuvieco et al. 2004a). Extremely low results were found in the correlation between DFMC and NDVI (Figure 4d). Specifically, the coefficient of determination was very low ($r^2 = 0.01$) without any statistical significance ($P > 0.05$). These results were expected, since according to Chuvieco et al. (2004a), the vegetation index does not measure the variations of moisture content directly but it estimates its effects on chlorophyll that may not be necessarily related. However, besides the very low results, it is worth noting that the correlation was found negative. This negative relationship between FMC and NDVI does not correspond to the assumptions made by many authors.

Since the initial correlation did not have the expected results, it was decided to test if the 10-f fuel moisture content is correlated with the top of atmosphere brightness temperature of Landsat 8 thermal bands. In this case, the results were much more satisfactory considering the assumptions made in the introduction of the study. In these models, the Mytilene RAWS was also included since the lack of LST values does not influence the regression. In this correlation both of the brightness temperature bands were tested. The correlation between DFMC and BT1 resulted to an r^2 = 0.733, while the usage of BT2 as an independent variable resulted to an r^2 = 0.65. Scatterplots of these regressions are shown on Figure 5. Statistical significance was found in both models ($P < 0.05$) with negative relationship confirming that higher temperatures reduce the moisture content. Taking into account these results it seems that top of atmosphere brightness temperature measured from satellite sensors has statistically significant results when correlated with real 10-h FMC measurements from RAWS. To explain the relationship of brightness temperature with fuel moisture content, and especially with DFMC, the details of retrieving the LST from brightness temperature should be explored. Many researchers have developed different ways for the retrieval of LST through the years by using satellite sensors. Yu et al. (2014) described further these methods for the TIR bands of Landsat 8. As mentioned before, sensors measure radiances reaching the satellite level and BT can be derived, so LST estimation algorithms can use brightness temperature as input (Dash et al., 2002).

In general, BT is atmospheric dependent, measured at satellite level and is lower than the actual LST. Usually, the difference between BT and LST in the 10-12 μm region is 1 to 5 K (Prata et al., 1995). Therefore, if the atmospheric effect and the surface spectral emissivity is taken into account, observed brightness temperature can provide LST with various algorithms (Dash et al., 2002). The importance of the atmospheric effects is noted also by many authors (Cristobal et al., 2009; Chrysoulakis and Cartalis, 2010; Ignatov and Dergileva, 1994) mentioning that deriving LST using BT is feasible under cloud free data. However, the derivation of LST with these known parameters is not enough because complex procedures are used to determine actual earth temperature.

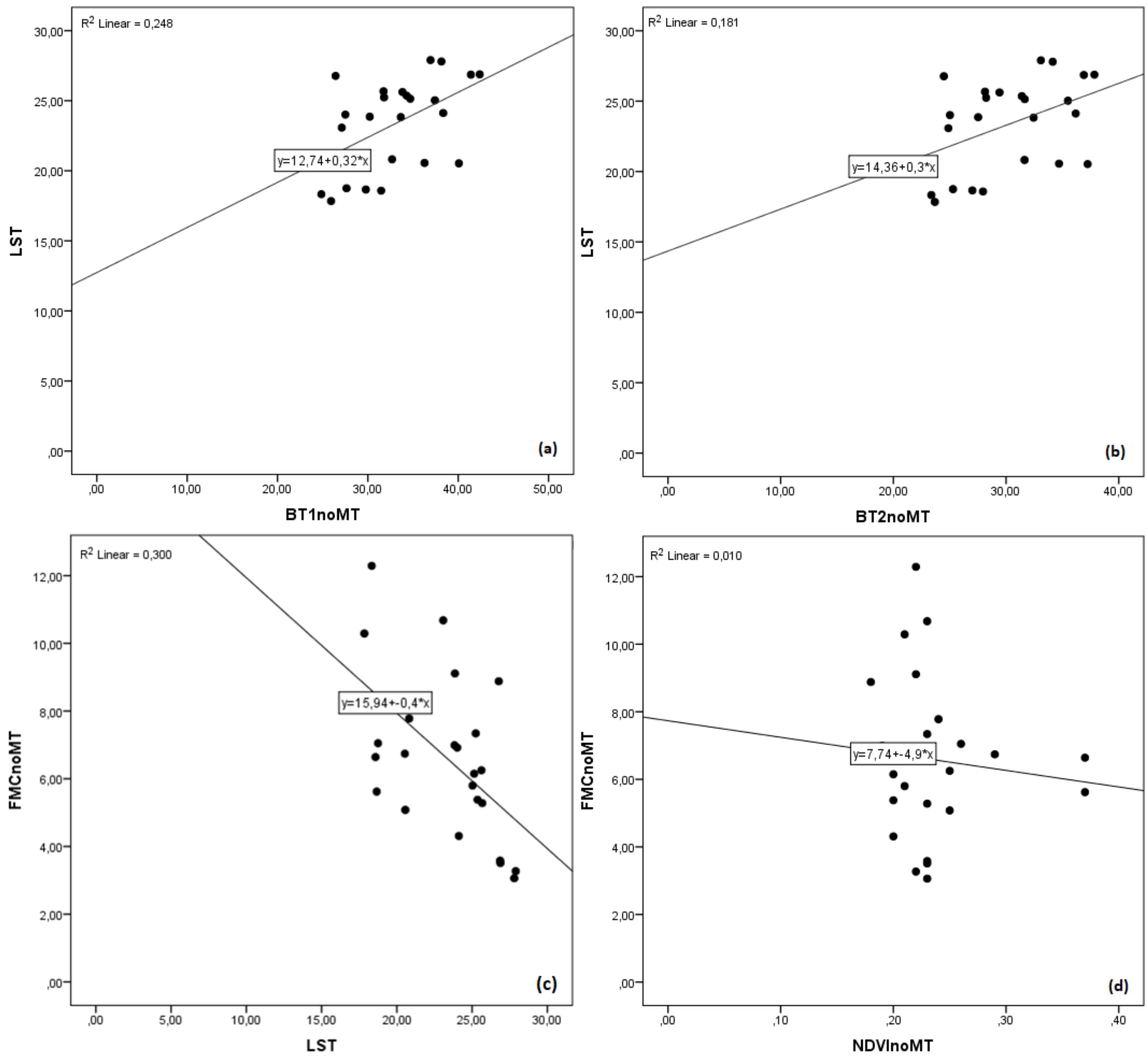

Figure 4: Scatterplots of (a) LST/BT1, (b) LST/BT2, (c) FMC/LST and (d) FMC/NDVI.

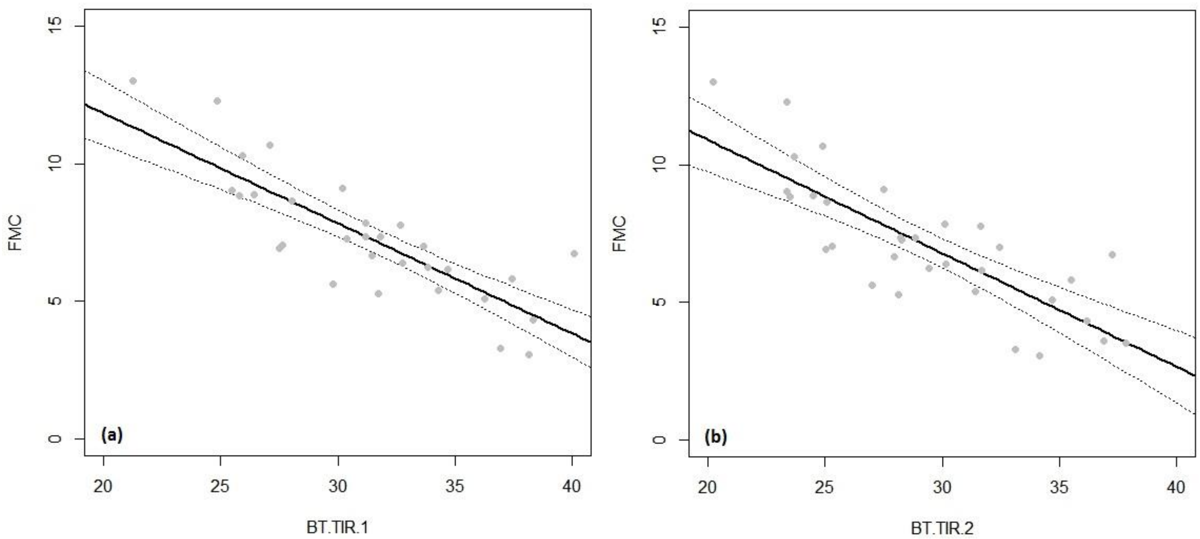

Figure 5: Scatterplots of (a) FMC/BT1 and (b) FMC/BT2 with the lower and upper confidence limits (95%)

These assumptions can confirm the relationship of DFMC and brightness temperature as both of them are affected from atmospheric conditions. Nevertheless, because none of the regressions models initially assumed in the methodology were effective except those combining DFMC and BT, it was decided to keep the one with the most significant results. Therefore, the final equation to estimate the DFMC from Landsat 8 satellite data is the following:

$$DFMC = 19.832 - 0.4 \times BT1 \tag{9}$$

3.2 Validation of the results

To validate the results, nine Landsat 8 images of the 2016 wildfire period were used. For the same days and hours of acquisition, the actual values of DFMC from RAWS were retrieved and compared with the estimated values of DFMC, computed based on top of atmosphere BT1 band of Landsat images by using the equation 9. The scatterplot of the residuals versus predicted DFMC values is symmetrically distributed, tending to cluster towards the middle of the plot and around the zero value of y-axis, while it does not present clear patterns (Figure 6a). Also, from the histogram of residuals (Figure 6b) it seems that the variance is almost normally distributed. The calculated root mean square (RMS) error was 1.477 according to the equation:

$$RMS = \sqrt{\frac{\sum_{i=1}^{n}(\hat{y}_i - y_i)^2}{n}} \tag{10}$$

where, n is the number of observations, $\hat{y}$ are the predicted DFMC values from Landsat and y are the DFMC values from RAWS.

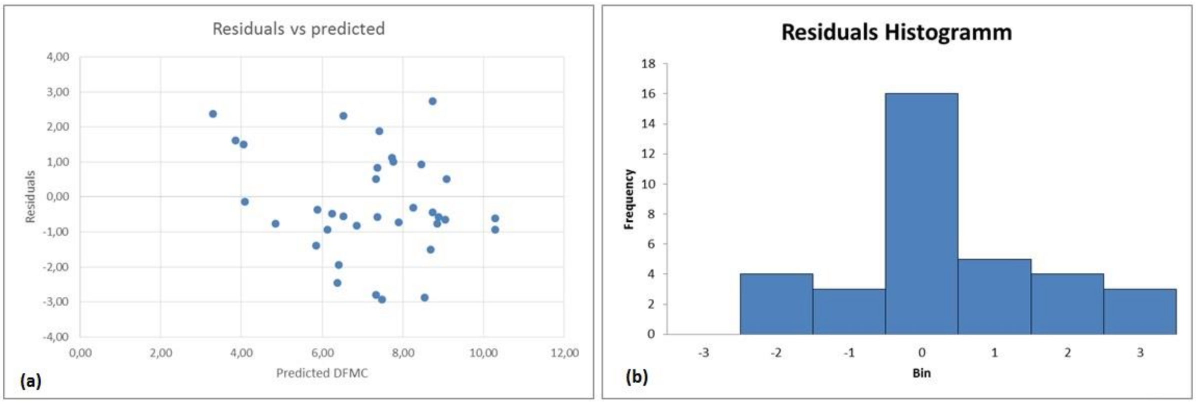

Figure 6: (a) Scatterplot of residuals versus predicted DFMC and (b) residuals histogram for the validation period of 2016.

Regarding the automated procedure for the DFMC creation, each new order requires approximately 2 hours for completion. To enable the sharing of information easily and promptly, the output files are accessible through a web-based front end that, eliminates the need to install special desktop software. This enables any authorized user to immediately access the platform from anywhere in the world. Users have the ability, without the requirement of knowing the handling of commercial and complicated GIS applications, to view the latest created DFMC files or view older DFMC files which are stored in the DFMC archive. Output files are also available for download to perform any meta-analysis. In this context, a set of maps was prepared to validate the spatial and the temporal distribution of the DFMC in the study area (Figures 7-10).

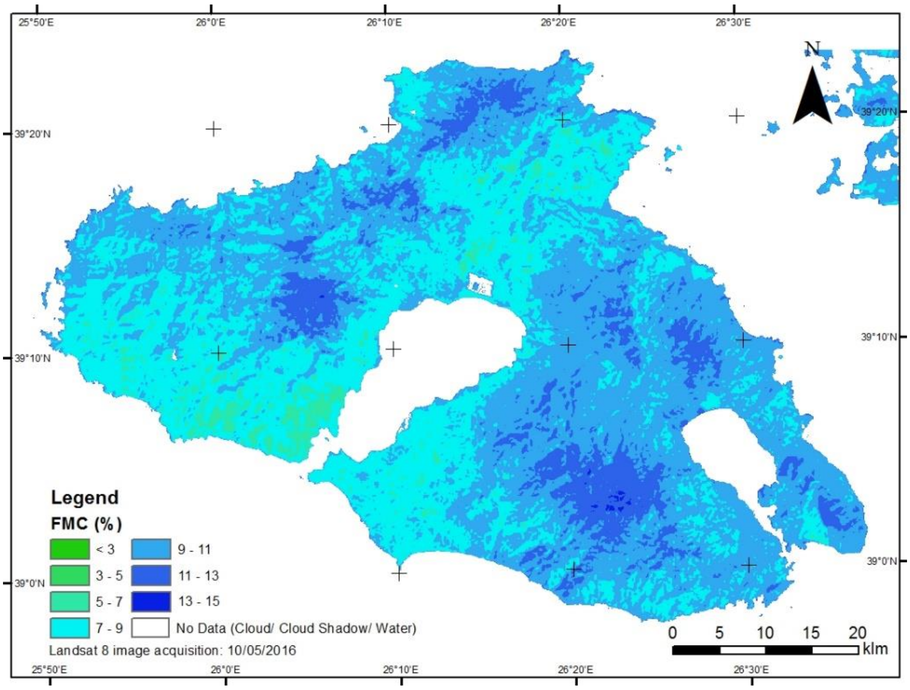

Figure 7: 10-h fuel moisture content estimation of Lesvos Island based on Landsat 8 top of atmosphere brightness temperature for 10-05-2016.

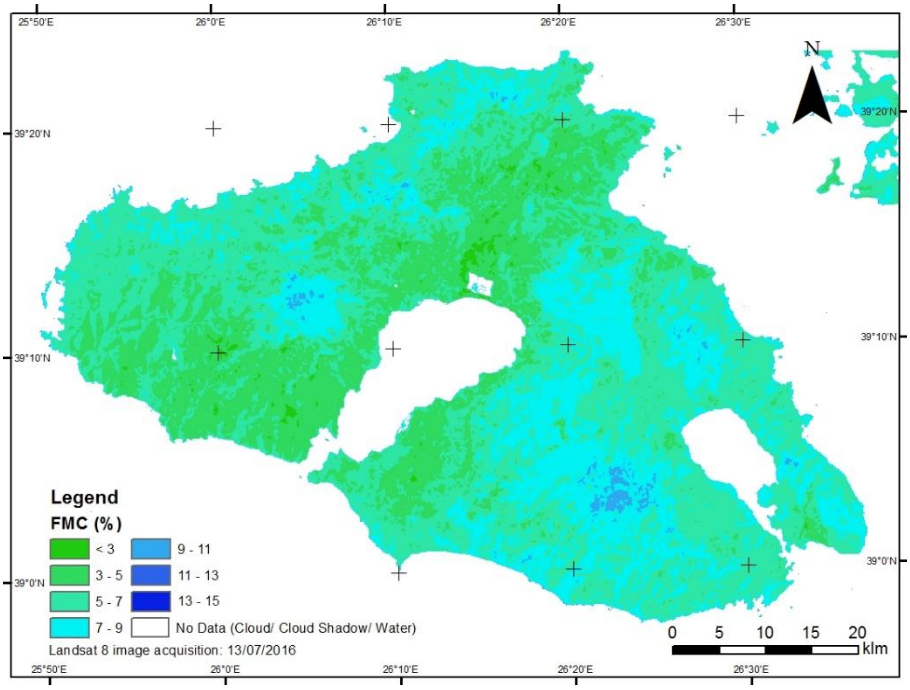

Figure 8: 10-h fuel moisture content estimation of Lesvos Island based on Landsat 8 top of atmosphere brightness temperature for 13-07-2016

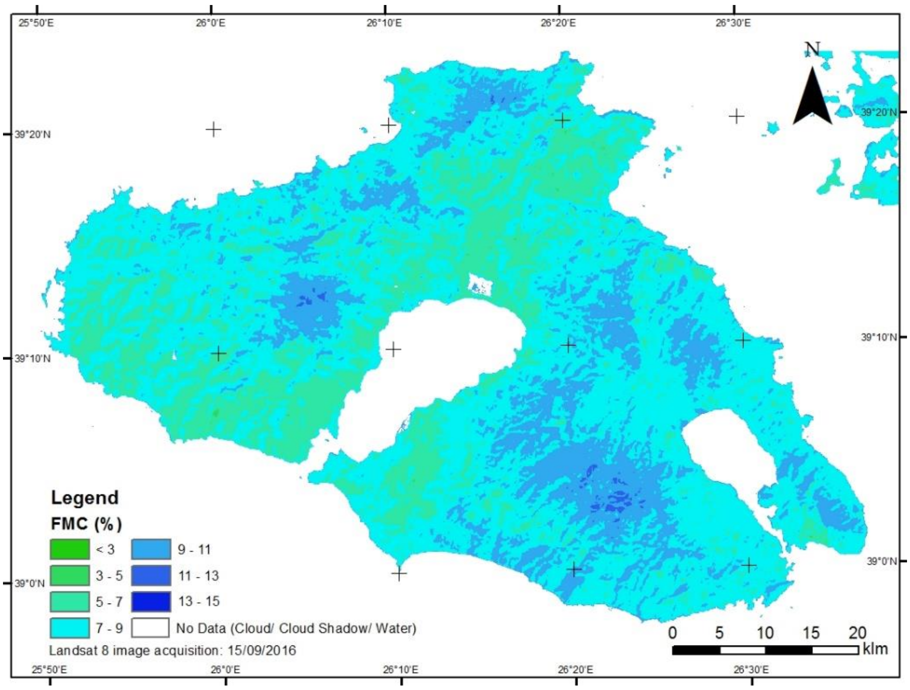

Figure 9: 10-h fuel moisture content estimation of Lesvos Island based on Landsat 8 top of atmosphere brightness temperature for 15-09-2016

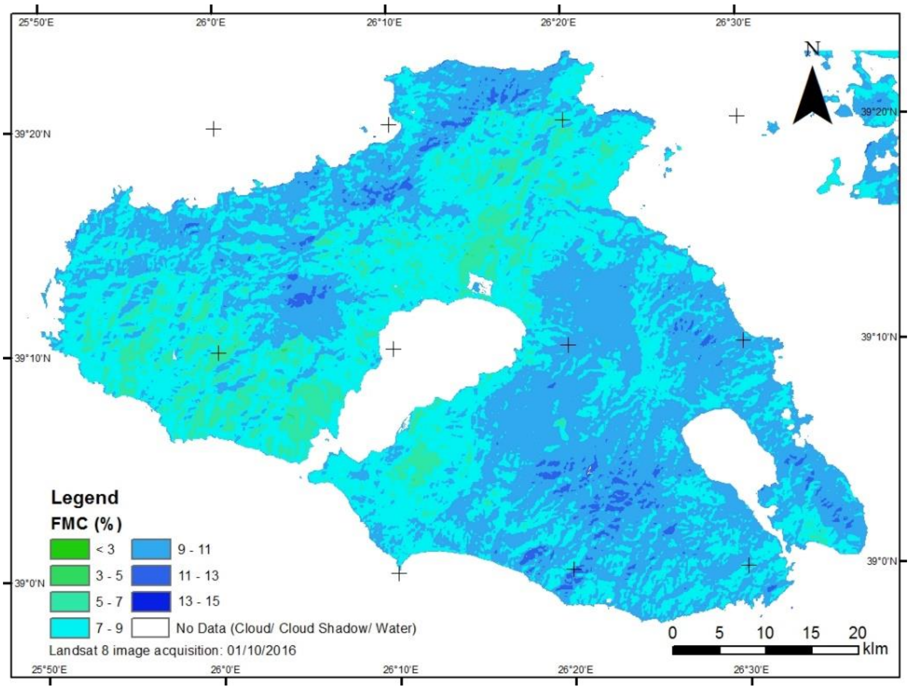

Figure 10: 10-h fuel moisture content estimation of Lesvos Island based on Landsat 8 top of atmosphere brightness temperature for 01-10-2016

4. CONCLUSIONS

In this paper, remote sensing techniques where applied to explore any linear relationships between 10-hour fuel moisture content and satellite multispectral data. Although many studies have shown that there is a significantly linear correlation between FMC and NDVI - LST ratio, results of the specific regression were not as expected in our study. Other studies

were conducted by using more data in a wider spatial extent and for different vegetation types and various satellite indices and sensors. However, in our study it was found that there is a good linear correlation between real data of 10-hour DFMC and the top of atmosphere brightness temperature computed from multispectral image processing. Also, the validation results for year 2016 by using data that were not considered within the regression modelling were quite noteworthy. Therefore, we can conclude that an accepted spatial estimation of the DFMC can be computed based on the brightness temperature of Landsat 8 without any atmospheric correction. Also, the temporal variation is significant as it depicts the DFMC variations within a wildfire period.

Further analysis can include data from a wider period and by testing other indices, i.e. Normalized Difference Water Index (NDWI) and the Normalized Difference Infrared Index (NDII) which is a widely-used index to remotely sense Equivalent Water Thickness (EWT) of leaves and canopies. Nonlinear curve estimations also could be tested. It is clear the importance of using both ground and satellite measurements for estimating and predicting fire behavior because wildfires are connected directly to vegetation moisture content. Specifically, DFMC has proved to be more important in such studies, due to lack of moisture compared to live FMC (Chuvieco et al., 2004b). Besides Landsat 8, new sensors with higher temporal, spectral and spatial resolution i.e. (Sentinel 2) can be explored to retrieve indices that will be more sensitive to the water content.

ACKNOWLEDGEMENTS

Landsat Surface Reflectance products courtesy of the U.S. Geological Survey. Landsat Spectral Indices products courtesy of the U.S. Geological Survey Earth Resources Observation and Science Center.

REFERENCES

Aguado, I., Chuvieco, E., Born, R. and Nieto, H. 2007. Estimation of dead fuel moisture content from meteorological data in Mediterranean areas. Applications in fire danger assessment. *International Journal of Wildland Fire* 16(4): 390 – 397.

Alosno, M., Camarasa, A., Chuvieco, E., Cocero, D., Kyun, I., Martin, M. P. and Salas, F. J. 1996. Estimating temporal dynamics of fuel moisture content of FMC of Mediterranean species from NOAA-AVHRR data. *EARSeL Advances in Remote Sensing* 4(4): 9 – 24.

Ceccato, P., Flasse, S., Tarantola, S., Jacquemoud, S. and Gregoirea, J. M. 2001. Detecting vegetation leaf water content using reflectance in the optical domain. *Remote Sensing of Environment* 77: 22 – 33.

Chrysoulakis, N. and Cartalis, C. 2010. A new approach for the detection of major fires caused by industrial accidents, using NOAA/AVHRR imagery. *International Journal of Remote Sensing* 21(8): 1743 – 1748.

Chuvieco, E., Riano, D., Aguado, I. and Cocero, D. 2002. Estimation of fuel moisture content from multitemporal analysis of Landsat Thematic Mapper reflectance data: applications in fire danger assessment. *International Journal of Remote Sensing* 23(11): 2145 – 2162.

Chuvieco, E., Cocero, D., Riaño, D., Martin P., Martinez-Vega, J., De la Riva, J. and Perez, F. 2004a. Combining NDVI and surface temperature for the estimation of live fuel moisture content in forest fire danger rating. *Remote Sensing of Environment* 92: 322 – 331.

Chuvieco, E., Cocero, D., Aguado, I., Palacios, A. and Prado, E. 2004b. Improving burning efficiency estimates through satellite assessment of fuel moisture content. *Journal of Geophysical Research* 109(14): 1 – 8.

Chuvieco, E (ed.). 2009. Earth observation of wildland fires in Mediterranean ecosystems. Springer Ed., Dordrecht, The Netherlands.

Countryman, C. M. and Dean, W. A. 1979. *Measuring moisture content in living chaparral: a field user's manual*. USDA Forest Service General Technical Report PSW-036, 28 p.

Cristobal, J., Jimenez-Munoz, J. C., Sobrino, J. A., Ninyerola, M. and Pons, X. 2009. Improvements in land surface temperature retrieval from the Landsat series thermal band using water vapor and air temperature. *Journal of Geophysical Research* 114(D8): 2156 – 2202.

Danson, F. M. and Bowyer, P. 2004. Estimating live fuel moisture content from remotely sensed reflectance. *Remote Sensing of Environment* 92(3): 309 – 321.

Dasgupta, S., Qu, J. J. and Hao, X. 2005. Evaluating Remotely Sensed Live Fuel Moisture Estimations for Fire Behavior Predictions. EastFIRE conference 2005, George Mason University, Fairfax, VA.

Dash, P. Göttsche, F. M., Olesen, F. S. and Fischer, H. 2002. Land surface temperature and emissivity estimation from passive sensor data: Theory and practice-current trends. *International Journal of Remote Sensing* 23(13): 2563 – 2594.

Dimitrakopoulos, A. and Papaioannou, K.K. 2001. Flammability assessment of Mediterranean forest fuels. *Fire Technology* 37: 143–152.

Gao, B. C. 1996. NDWI – A Normalized Difference Water Index for Remote Sensing of Vegetation Liquid Water from Space. *Remote Sensing of Environment* 58: 257 – 266.

Gerdzheva, A. 2014. A comparative analysis of different wildfire risk assessment models (a case study for Smolyan district, Bulgaria). *European Journal of Geography* 5(3): 22 -36.

Hazaymeh, K. and Hassan, Q. K. 2015. Fusion of MODIS and Landsat-8 Surface Temperature Images: A New Approach. *PLoS ONE* 10(3): 1 – 13.

Hong, S., Lakshmi, V. and Small, E. E. 2007. Relationship between vegetation biophysical properties and surface temperature using multisensor satellite data. *Journal of Climate* 20: 5593 – 5606.

Ignatov, A. M. and Dergileva, I. L. 1994. Angular effect in dual-window AVHRR brightness temperatures over oceans. *International Journal of Remote Sensing* 15(18): 3845 – 3850.

Jones, S. and Reinke, K. (eds.) 2009. Innovations in Remote Sensing and Photogrammetry Series: Lecture Notes in Geoinformation and Cartography. Springer: Berlin.

Li, Z-L., Tang, B-H., Wu, H., Ren, H., Yan, G., W, Z., Trigo, I. F. and Sobrino, J. A. 2013. Satellite-derived land surface temperature: Current status and perspectives. *Remote Sensing of Environment* 131: 14 – 37.

Masek, J.G., Vermote, E.F., Saleous, N., Wolfe, R., Hall, F.G., Huemmrich, F., Gao, F., Kutler, J. and Lim, T.K. 2006. A Landsat surface reflectance data set for North America, 1990-100, *IEEE Geoscience and Remote Sensing Letters* 3: 68-72.

Pinto, A., Espinosa – Prieto, J., Rossa, C., Matthews, S., Loureiro, C. and Fernandes, P. 2014. Modelling fine fuel moisture content and the likelihood of fire spread in blue gum (Eucalyptus globulus) litter. *Advances in Forest Fire Research*, (pp. 353 – 359). Coimbra University Press.

Pettorelli, N. 2013. The normalized difference vegetation index. Oxford University Press, New York. pp. 1 – 224.

Pollet, J. and Brown, A. 2007. Fuel Moisture Sampling Guide. Utah State Office, Bureau of Land Management, 1 – 30.

Prata, A. J., Caselles, V., Coll, C., Sobrino, J. A. and Ottlé, C. 1995. Thermal remote sensing of land surface temperature from satellites: Current status and future prospects. *Remote Sensing Reviews* 12: 175 – 224.

Prosper-Laget, V., Douguedroit, A. and Guinot, J. P. 1995. Mapping the risk of forest fire occurrence using NOAA satellite information. *EARSeL Advances in Remote Sensing 4*(3): 30 – 38.

Riaño, D., Vaughan, P., Chuvieco, E., Zarco-Tejada, P. J. and Ustin, S. L. 2005. Estimation of Fuel Moisture Content by Inversion of Radiative Transfer Models to Simulate Equivalent Water Thickness and Dry Matter Content: Analysis at Leaf and Canopy Level. *IEEE Transactions on Geoscience and Remote Sensing* 43(4): 819 – 826.

Rouse, J., Hass, R., Schell, J. and Deering, D. 1973. Monitoring vegetation systems in the great plains with ERTS. Third ERTS symposium, NASA, SP-351 I, p.309-317.

Sow, M., Mbow, C., Hély, C., Fensholt, R. and Sambo, B. 2013. Estimation of Herbaceous Fuel Moisture Content Using Vegetation Indices and Land Surface Temperature from MODIS Data. *Remote Sensing* 5*:* 2617 – 2638.

Sun, D. and Kafatos, M. 2007. Note on the NDVI-LST relationship and the use of temperature-related drought indices over North America. *Geophysical Research Letters* 34: 1 – 4.

Vejmelka, M., Kochanski, A. K. and Mandel, J. 2016. Data assimilation of dead fuel moisture observations from remote automated weather stations. *International Journal of Wildland Fire* 25(5): 558 – 568.

Verbesselt, J., Somers, B., Aardt, J., Jonckheere, I. and Coppin, P. 2006. Monitoring herbaceous biomass and water content with SPOT VEGETATION time-series to improve fire risk assessment in savanna ecosystems. *Remote Sensing of Environment* 101(3): 399 – 414.

Vermote, E., Justice, C., Claverie, M. and Franch, B. 2016. Preliminary analysis of the performance of the Landsat 8/OLI land surface reflectance product. *Remote Sensing of Environment* 185: 46-56.

Viegas, D. X., Pinol, J., Viegas, M. T. and Ogaya, R. 2001. Estimating live fine fuels moisture content using meteorologically-based indices. *International Journal of Wildland Fire* 10(2): 223 – 240.

Wan, Z., Wang, P. and Li, X. 2004. Using MODIS Land Surface Temperature and Normalized Difference Vegetation Index products for monitoring drought in the southern Great Plains, USA. *International Journal of Remote Sensing* 25(1): 61 – 72.

Yebra, M., Dennison, P. E., Chuvieco, E., Riaño, D., Zylstra P., Hunt Jr, E. R., Danson, F. M., Qi, Y. and Jurdao, S. 2013. A global review of remote sensing of live fuel moisture content for fire danger assessment: Moving towards operational products. *Remote Sensing of Environment* 136: 455 – 468.

Yu, X., Guo, X. and Wu, Z., 2014. Land surface temperature retrieval from Landsat 8 TIRS-comparison between radiative transfer equationbased method, split window algorithm and single channel method. *Remote Sensing* 6(10): 9829–9852.